METHOD FOR RECONSTRUCTION OF A DIELECTRIC CYLINDER DERIVED FROM A NOVEL OPERATOR EQUATION

Kenichi ISHIDA, Hiroyuki FURUKAWA and Mitsuo TATEIBA
Department of Computer Science and Communication Engineering,
Kyushu University
6-10-1 Hakozaki, Higashi-ku, Fukuoka-shi, Fukuoka 812-8581, Japan
E-mail ishida@csce.kyushu-u.ac.jp

1. Introduction

It is necessary to develop a reconstruction method of an object, sufficiently considering behavior of electromagnetic waves. In the previous studies, many iterative methods are reported[1–3]. They take much time to solve the direct scattering problem repeatedly. Additionally, if the initial guess of the object is close to the original one, we get the precise profile of the object through many iterations; otherwise fatal fault occurs because of local minimum problem. In this situation, the keys to solve the problem seem to be how to solve the direct problem quickly and how to escape from the local minimum points.

On the other hand, non-iterative methods have an advantage to give a solution within a certain time. Non-iterative methods are also important to give an initial guess also when the iterative methods are used. There is the famous non-iterative method by Born's approximation, but it is valid only for quite weak scattering object. Therefore an effective non-iterative is desired to be developed.

In this paper, we introduce an operator which relates the object and the scattered wave. From its operator equation, we derive a non-iterative method for reconstructing the object. Numerical examples are shown to investigate the validity of the approach.

2. Formulation

Let us consider reconstruction of a cylindrical inhomogeneous object located in a region $R_{\rm V}$ in free space from the scattered waves measured in a region $R_{\rm S}$ under E-wave time-harmonic excitations. The internal characteristics to be reconstructed is defined as the object function $o(\boldsymbol{r}) = k^2(n^2(\boldsymbol{r}) - 1)$, where k is the wavenumber in free space, and n is the refractive-index of the object. We denote the scattered wave by $u_{\rm s}$, incident waves by $u_{\rm in}$ and total waves by $u_{\rm t}$. These waves and the object function satisfy the well-known integral equations:

$$u_{\rm s}(\boldsymbol{r}) = \int_{R_{\rm V}} G(\boldsymbol{r}|\boldsymbol{r}')o(\boldsymbol{r}')u_{\rm t}(\boldsymbol{r}')\mathrm{d}\boldsymbol{r}', \quad \boldsymbol{r} \in R_{\rm S} \tag{1}$$

$$u_{\rm t}(\boldsymbol{r}) = u_{\rm in}(\boldsymbol{r}) + \int_{R_{\rm V}} G(\boldsymbol{r}|\boldsymbol{r}')o(\boldsymbol{r}')u_{\rm t}(\boldsymbol{r}')\mathrm{d}\boldsymbol{r}', \quad \boldsymbol{r} \in R_{\rm V} \tag{2}$$

where G is Green's function, and the time factor $\exp(-\mathrm{j}\omega t)$ is suppressed.

We introduce the operator T defined as

$$u_{\rm s}(\boldsymbol{r}) = \int_{R_{\rm V}}\int_{R_{\rm V}} G(\boldsymbol{r}|\boldsymbol{r}'')T(\boldsymbol{r}''|\boldsymbol{r}')u_{\rm in}(\boldsymbol{r}')\mathrm{d}\boldsymbol{r}''\mathrm{d}\boldsymbol{r}' \tag{3}$$

Comparing eq.(3) with eqs.(1) and (2), we obtain the following operator equation.

$$T(\boldsymbol{r}''|\boldsymbol{r}') = O(\boldsymbol{r}''|\boldsymbol{r}') + \int_{R_{\rm V}}\int_{R_{\rm V}} O(\boldsymbol{r}''|\boldsymbol{r}_1)G(\boldsymbol{r}_1|\boldsymbol{r}_2)T(\boldsymbol{r}_2|\boldsymbol{r}')\mathrm{d}\boldsymbol{r}_1\mathrm{d}\boldsymbol{r}_2 \tag{4}$$

where $O(\boldsymbol{r}''|\boldsymbol{r}_1)$ satisfies $\int_{R_{\rm V}} O(\boldsymbol{r}''|\boldsymbol{r}_1)u(\boldsymbol{r}_1)\mathrm{d}\boldsymbol{r}_1 = o(\boldsymbol{r}'')u(\boldsymbol{r}'')$ for any wave function $u(\boldsymbol{r}'')$. We can see from eqs.(3) and (4) that if T is estimated through eq.(3), then $o(\boldsymbol{r})$ is reconstructed from a linear equation (4).

On the basis of the equations, we consider a method for reconstruction. The object function $o(\boldsymbol{r})$ is assumed to be expanded by orthogonal functions $\phi_l(\boldsymbol{r})$ as $o(\boldsymbol{r}) = \sum_{l=1}^{\infty} o_l\phi_l(\boldsymbol{r})$.

Then we get

$$O(\boldsymbol{r}''|\boldsymbol{r}') = \sum_{l=1}^{\infty} o_l \phi_l(\boldsymbol{r}'')\delta(\boldsymbol{r}''|\boldsymbol{r}') \tag{5}$$

where δ is the delta function. In general, a certain set of incident waves $u_{\rm in}^{(q)}(\boldsymbol{r}')$ illuminates the object successively and the scattered waves are measured on a certain point $\boldsymbol{r}_m$. Operating $G(\boldsymbol{r}_m|\boldsymbol{r}'')$ and $u_{\rm in}^{(q)}(\boldsymbol{r}')$ to eq.(4) and substituting eq.(5) into eq.(4), we get

$$\begin{aligned}
&\int_{R_{\rm V}}\int_{R_{\rm V}} G(\boldsymbol{r}_m|\boldsymbol{r}'')T(\boldsymbol{r}''|\boldsymbol{r}')u_{\rm in}^{(q)}(\boldsymbol{r}')\mathrm{d}\boldsymbol{r}''\mathrm{d}\boldsymbol{r}' \\
&= \sum_{l=1}^{\infty} o_l \Big[\int_{R_{\rm V}} G(\boldsymbol{r}_m|\boldsymbol{r}')\phi_l(\boldsymbol{r}')u_{\rm in}^{(q)}(\boldsymbol{r}')\mathrm{d}\boldsymbol{r}' \\
&\quad + \int_{R_{\rm V}}\int_{R_{\rm V}}\int_{R_{\rm V}} G(\boldsymbol{r}_m|\boldsymbol{r}_1)\phi_l(\boldsymbol{r}_1)G(\boldsymbol{r}_1|\boldsymbol{r}_2)T(\boldsymbol{r}_2|\boldsymbol{r}')u_{\rm in}^{(q)}(\boldsymbol{r}')\mathrm{d}\boldsymbol{r}_1\mathrm{d}\boldsymbol{r}_2\mathrm{d}\boldsymbol{r}'\Big]
\end{aligned} \tag{6}$$

Using the relation $\delta(\boldsymbol{r}''|\boldsymbol{r}') = \sum_{l=1}^{\infty} \phi_l(\boldsymbol{r}'')\frac{1}{\Lambda_l}\phi_l^*(\boldsymbol{r}')$ with $\Lambda_l = \int_{R_{\rm V}} \phi_l^*(\boldsymbol{r}')\phi_l(\boldsymbol{r}')\mathrm{d}\boldsymbol{r}$, we can finally reduce eq.(6) into an equation for o_l as follows:

$$\mathcal{P}_{mq} = \sum_{l=1}^{\infty} o_l \Big[\bar{\mathcal{B}}_{mq}^{l} + \sum_{l_2=1}^{\infty}(\sum_{l_1=1}^{\infty}\mathcal{M}_{ml_1}\bar{\mathcal{G}}_{l_1l_2}^{l})\mathcal{C}_{l_2q}\Big] \tag{7}$$

where

$$\mathcal{P}_{mq} = \int_{R_{\rm V}}\int_{R_{\rm V}} G(\boldsymbol{r}_m|\boldsymbol{r}'')T(\boldsymbol{r}''|\boldsymbol{r}')u_{\rm in}^{(q)}(\boldsymbol{r}')\mathrm{d}\boldsymbol{r}''\mathrm{d}\boldsymbol{r}' \tag{8}$$

$$\bar{\mathcal{B}}_{mq}^{l} = \int_{R_{\rm V}} G(\boldsymbol{r}_m|\boldsymbol{r}')\phi_l(\boldsymbol{r}')u_{\rm in}^{(q)}(\boldsymbol{r}')\mathrm{d}\boldsymbol{r}' \tag{9}$$

$$\mathcal{M}_{ml_1} = \int_{R_{\rm V}} G(\boldsymbol{r}_m|\boldsymbol{r}_1)\phi_{l_1}(\boldsymbol{r}_1)\mathrm{d}\boldsymbol{r}_1 \tag{10}$$

$$\bar{\mathcal{G}}_{l_1l_2}^{l} = \int_{R_{\rm V}}\int_{R_{\rm V}} \frac{1}{\Lambda_{l_1}}\phi_{l_1}^*(\boldsymbol{r}_1)\phi_l(\boldsymbol{r}_1)G(\boldsymbol{r}_1|\boldsymbol{r}_2)\phi_{l_2}(\boldsymbol{r}_2)\mathrm{d}\boldsymbol{r}_1\mathrm{d}\boldsymbol{r}_2 \tag{11}$$

$$\mathcal{C}_{l_2q} = \int_{R_{\rm V}}\int_{R_{\rm V}} \frac{1}{\Lambda_{l_2}}\phi_{l_2}^*(\boldsymbol{r}_2)T(\boldsymbol{r}_2|\boldsymbol{r}')u_{\rm in}^{(q)}(\boldsymbol{r}')\mathrm{d}\boldsymbol{r}_2\mathrm{d}\boldsymbol{r}' \tag{12}$$

where $\mathcal{C}_{lq}$ is the equivalent current and satisfies the equation

$$\mathcal{P}_{mq} = \sum_{l=1}^{\infty}\mathcal{M}_{ml}\mathcal{C}_{lq} \tag{13}$$

Comparing eq.(8) with eq.(3), we can see that $\mathcal{P}_{mq}$ is the measured data. The algorithm to solve eq.(7) can be summarized as follows:

Step 0 Calculate $\bar{\mathcal{B}}$, $\bar{\mathcal{G}}$, $\mathcal{M}$. This step can be done in advance because they are independent of the scattered wave.
Step 1 Calculate $\mathcal{C}$ from eq.(13).
Step 2 Align the elements with subscript m, q of eq.(7) in a single column to obtain a matrix equation. Calculate o from the matrix equation.

In passing, it is worth noting that we can also obtain the equivalent current method[4] and unrelated illumination method[5] from the operator equation(4) by choosing the operating functions.

3. Numerical results

We use a configuration shown in Fig. 1 in the following numerical examples for simplicity. We assume that the incident waves are plane waves which propagate in Q different directions and that the complex(amplitude and phase) scattered far-waves are received in M different directions. That is,

$$u_{\rm in}^{(q)}(\boldsymbol{r}) = \exp(-\mathrm{j}k\boldsymbol{i}_q\cdot\boldsymbol{r}),\ q=1,\cdots,Q;\quad G(\boldsymbol{r}_m|\boldsymbol{r}) \sim -\frac{\mathrm{j}}{4}\exp(+\mathrm{j}k\boldsymbol{s}_m\cdot\boldsymbol{r}),\ m=1,\cdots,M \tag{14}$$

where $\boldsymbol{s}_m = (\cos\theta_m, \sin\theta_m)$, $\boldsymbol{i}_q = (\cos\phi_q, \sin\phi_q)$ are unit vectors which indicate the direction of observation and illumination, respectively. The size of the region $R_{\rm V}$ is set to $2R \times 2R$, and ϕ_l is chosen as a pulse function, which exists over only l-th small cell which is made by dividing the region $R_{\rm V}$ vertically and horizontally by L. Then, the series of l in eqs.(7) and (13) are changed to the partial sums for $l = 1, \cdots, L$. Under the above setting, we can analytically calculate the matrices in eqs.(8)–(11).

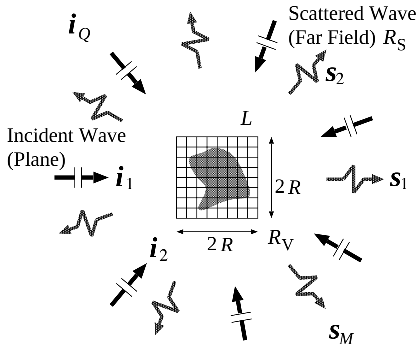

Figure 1: Geometry.

At first, we consider the reconstructions of a cylinder of the different radius and different refractive-index. Figure 2 shows the reconstructed profile of a cylinder of radius 1.0λ(λ is the wavelength) with different refractive index, where $R = 1.2\lambda$, $L = 576$. In this calculation, eq.(7) is solved by the truncated singular value decomposition(TSVD), where the truncation is empirically done. Figure 3 shows the reconstructed profile of a cylinder of refractive index $n^{\rm org} = 1.1$ with different radius, where R is set $1.2a$(a is the radius of the original cylinder) and L is set proportionately with the area of $R_{\rm V}$. We can see from the result that our approach seems applicable for a cylinder with $n^{\rm org} \leq 1.1$ if $a = 1.0\lambda$ or with $a \leq 1.0\lambda$ if $n^{\rm org} = 1.1$. This applicability limit is the same as the modified Newton-Kantrovich method[6], which is one of iterative methods.

Next, we use the Tikhonov regularization(TR) to solve eq.(7), where the regularization parameter is chosen by the generalized cross-validation method[7]. The reconstructed profiles is shown in Fig. 4. We can see that the profiles is better than that by TSVD. Progress for the applicability limit is, however, not achieved well.

At last, we consider the reconstruction from noisy scattered waves. Figure 5 shows the reconstructed profiles for different SNR. We can manage to see the object even if SNR is 15dB. Figure 6 shows the root-mean square error of reconstructed profile by TSVD and TR. In this case, TR produces the better profile than TSVD when SNR is not low.

4. Conclusion

We have been derived a non-iterative method for reconstruction of a cylinder from an operator equation. Numerical simulation has been done for a lossless cylinder using the truncated singular value decomposition or using Tikhonov's regularization technique. It shows that our non-iterative approach is applicable for a cylinder with the same inhomogeneity as the modified Newton-Kantrovich method. Tikhonov's regularization technique is more useful in calculating the resultant matrix equation.

We can obtain different methods from the operator equation by choosing the different operating functions in the same manner. Derivation of an excellent method by operating some adequate functions is a future work.

Acknowledgement

This work was supported in part by Grant-In-Aid for Scientific Research(10750322) from the Ministry of Education, Science, Sports, and Culture, Japan.

References

[1] H. Harada, D. J. N. Wall, T. Takenaka, and M. Tanaka. *IEEE Trans. Antennas & Propag.*, Vol. 43, No. 8, pp. 784–792, 1995.

[2] K. Ishida and M. Tateiba. *Proc. SPIE*, Vol. 3171, pp. 186–197, July 1997.

[3] R. V. McGahan and R. E. Kleinman. *IEEE Antennas Propag. Magazine*, Vol. 41, No. 1, pp. 34–51, 1998.

[4] S. Caorsi, G. L. Gragnani, and M. Pastorino. *IEE Proc.-H*, Vol. 139, No. 1, pp. 45–52, 1992.

[5] W. Wang and S. Zhang. *IEEE Trans. Antennas & Propag.*, Vol. 40, No. 11, pp. 1292–1296, 1992.

[6] T. Takenaka, H. Harada, and M. Tanaka. *Micro. Opt. Tech. Lett.*, Vol. 5, No. 2, pp. 94–97, February 1992.

[7] G. H. Golub, M. Heath, and G. Wahba. *Technometrics*, Vol. 21, No. 2, pp. 215–223, 1979.

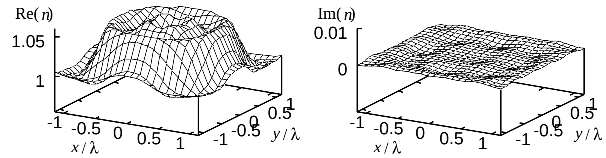

(a) $n^{\text{org}} = 1.05 - \text{j}0.0$, radius: 1.0λ

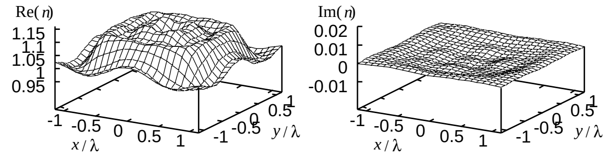

(b) $n^{\text{org}} = 1.1 - \text{j}0.0$, radius: 1.0λ

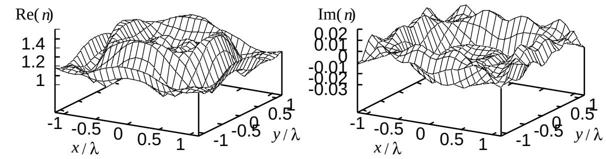

(c) $n^{\text{org}} = 1.2 - \text{j}0.0$, radius: 1.0λ

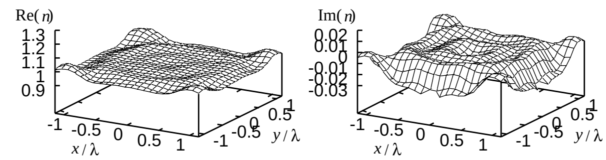

(d) $n^{\text{org}} = 1.3 - \text{j}0.0$, radius: 1.0λ

Figure 2: Reconstruction of a cylinder with different refractive-index from noiseless scattered waves by means of TSVD.

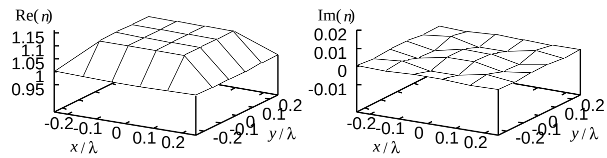

(a) $n^{\text{org}} = 1.1 - \text{j}0.0$, radius: 0.25λ

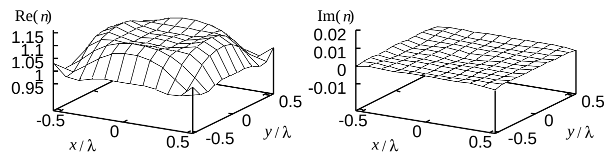

(b) $n^{\text{org}} = 1.1 - \text{j}0.0$, radius: 0.5λ

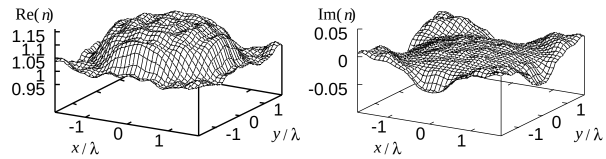

(b) $n^{\text{org}} = 1.1 - \text{j}0.0$, radius: 1.5λ

Figure 3: Reconstruction of a cylinder with different radius from noiseless scattered waves by means of TSVD.

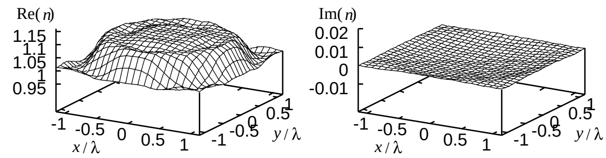

(a) $n^{\text{org}} = 1.1 - \text{j}0.0$, radius: 1.0λ

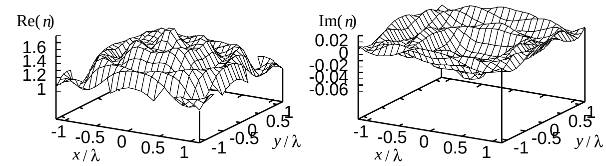

(b) $n^{\text{org}} = 1.2 - \text{j}0.0$, radius: 1.0λ

Figure 4: Reconstruction of a cylinder from noiseless scattered waves by means of TR.

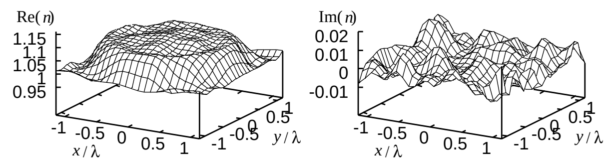

(a) $n^{\text{org}} = 1.1 - \text{j}0.0$, radius: 1.0λ, SNR=30dB

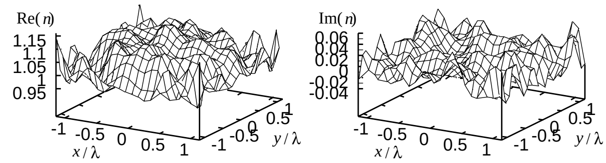

(b) $n^{\text{org}} = 1.1 - \text{j}0.0$, radius: 1.0λ, SNR=15dB

Figure 5: Reconstruction of a cylinder from noisy scattered waves by means of TR.

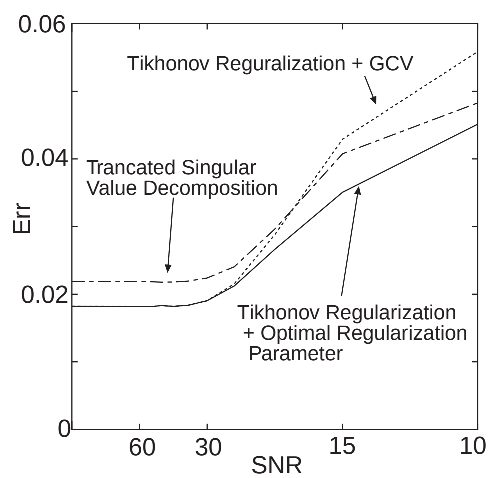

Figure 6: Root-mean-square error of reconstructed refractive-index profile Err for a cylinder of $n^{\text{org}} = 1.1 - \text{j}0.0$ and radius 1.0λ.